17th World Conference on Earthquake Engineering, 17WCEE
Sendai, Japan - September 13th to 18th 2020

COLLAPSE TIME OF REINFORCED CONCRETE BUILDINGS CONSIDERING SUCCESSIVE EARTHQUAKES

Y. Guo[(1)], T. Nakamura[(2)]

[(1)] *Graduate student, Graduate School of Science and Technology Niigata University, itoumomogyj@gmail.com*
[(2)] *Associate Professor, Faculty of Eng., Niigata University, takaya@eng.niigata-u.ac.jp*

Abstract

This study focuses on the story collapse of reinforced concrete (RC) buildings with brittle columns. After a building is damaged by a large earthquake, it is important to evaluate the effect of subsequent ground motions. In addition, the time required for such buildings to collapse must be known for evacuation planning. Thus, by conducting a dynamic analysis, this study aims to examine the collapse time of RC buildings considering the effect of large successive earthquakes.

Three- and nine-story RC buildings designed according to old Japanese codes (codes established before 1971) were analyzed. The buildings were represented by equivalent shear building models. The third story from the top was selected as the collapse story. Thus, nine-story buildings suffered an intermediate-story collapse; this has, often been observed in the past in old medium-rise buildings during severe earthquakes. We assumed that only a single story collapsed, and the damage induced by past earthquakes on other stories was negligible.

The relationship between the lateral load and inter-story drift in the model was represented by a quadrilinear function based on previously conducted collapse tests of brittle columns. Strength deterioration after a maximum load was considered. A dynamic analysis was performed for various columns and ground motions. It is important to calculate the residual time to collapse after oscillations in a building are first perceived as this determines the amount of time a person has to evacuate the building. This time interval is referred to as “collapse time”. The levels of first ground motions were adjusted, and second ground motions were successively input. The ground motion levels were adjusted to induce collapse in order to identify the collapse time. In addition, the relationship between the maximum drift in the first ground motion and the collapse time in the second ground motion was discussed.

The study reveals that in most cases, the collapse time was very short for individuals to safely evacuate a building. Further, the collapse time depended on the relationship between the elongation of the natural period of buildings due to the large plastic response in the first ground motion and the period of the second ground motion.

Keywords: Reinforced Concrete Buildings, Collapse Time, Successive Earthquake

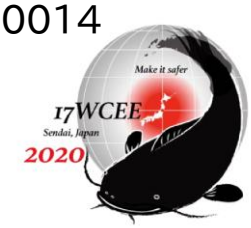

1. Introduction

At present, several vulnerable buildings designed according to pre-1971 Japanese building codes still remain. Among them, reinforced concrete (RC) buildings with brittle columns are considered to have a high risk of story collapse and are the focus of this study. Once buildings are damaged by a large earthquake, it is important to evaluate the effect of subsequent ground motions [1,2,3]. In addition, the time required for such buildings to collapse must be known for evacuation planning. This study aims to examine the collapse time of RC buildings considering large successive earthquakes by conducting a dynamic analysis. Three- and nine-story buildings were analyzed, and the responses of the model buildings in post-peak regions, including collapse, were studied. In addition, the relationship between the maximum drift in the first ground motion and the collapse time in the second ground motion was discussed, and the effects of a predominant period of ground motion (short-period or long-period) and the collapse time were assessed.

2. Outline of analysis

2.1 Analytical model

In this study, RC buildings designed according to old Japanese codes (codes established before 1971) were analyzed. In 1971, the regulations for transverse reinforcement ratios were strengthened. This study analyzes buildings with three and nine stories, with a focus on three-story buildings. The steps in the analysis are outlined below.

(1) The buildings are represented by equivalent shear building models. The analytical models of a three-story building and a nine-story building are shown in Fig. 1. They are designed to comprise a single column line and a rigid beam. Conventional member to member analysis cannot be used here because it is currently impossible to realistically represent column axial behavior at and after collapse. The height and weight of each story are assumed to be 3600 mm and 753 kN, respectively. The structural properties of the analytical models of the three-story and nine-story buildings are summarized in Table 1, indicated by (a) and (b), respectively.

(2) The building model consists of a brittle column (clear height h_0 = 2400 mm, column section width b * depth D = 600 mm * 600 mm, and h_0/D = 4). Fig. 2 shows an idealized column, which is assumed to be twice as large as the tested specimens [4].

(3) The story strength distribution is determined based on a uniform design load distribution prescribed by pre-1971 Japanese building codes. However, according to common construction practice, the column sizes of the top two or three stories are the same; therefore, it is assumed that all stories of the three-story building have the same strength, while the top three stories of the nine-story building have the same strength. We also assumed that past earthquakes only caused a single story to collapse and damage to other stories was negligible: the collapsed story was assumed to be weaker than the other stories. The third story from the top is selected as the “collapse story” for the analysis and its strength is reduced to 80% of the previously determined strength. Fig. 3 compares the story strength distribution of the analytical model and the lateral strength required by the Japanese building code for a nine-story building. As a result, the model buildings are expected to collapse near the third story from the top. As such, three- and nine-story buildings suffered collapses, at their first and seventh stories, respectively. Thus, the nine-story buildings were considered to suffer the intermediate-story collapse that occurred during the 1995 Kobe earthquake.

(4) The seismic capacity index, I_S, is computed for each story using the second-level procedure described in the Standard for Seismic Evaluation [5,6]. The strength of each story is determined such that the value of I_S for the collapse story is 0.4. In Japan, the value of I_S is commonly used to evaluate the seismic performance of existing RC buildings. It is widely recognized that when $I_S \geqq 0.6$, such buildings do not suffer serious damage or collapse even during severe earthquakes. Note that the I_S value for buildings designed under the Japanese building code is generally 0.4 [7]. As described in the Appendix, the I_S value is calculated based on the product of the strength index C and the deformability index F. The index C is defined as the strength of a

column divided by the total weight of floors above the column, and the index F is determined based on the deformability of a column. The F values of columns that are twice the size of the tested samples are computed to be 1.0. Because of the assumed distribution of story strength, I_S takes its lowest value at the collapse story. Hereinafter, I_S for the collapse story is considered to be applicable to the entire building.

(5) The initial distribution of story stiffness is the same as the story strength distribution. The initial stiffness of each story is such that the first mode periods are 0.22 s and 0.65 s for the three- and nine-story buildings, respectively. They are computed using the standard equation $T = 0.22\ h$, where h is the total height of the building in meters.

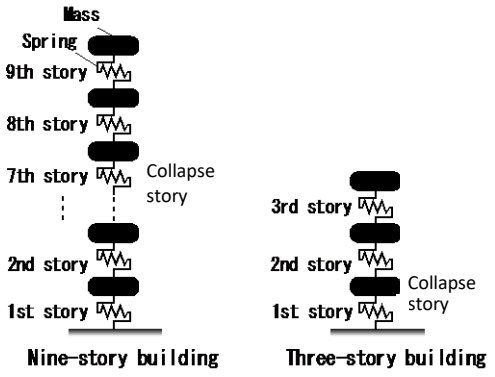

Fig.1 – Analytical models

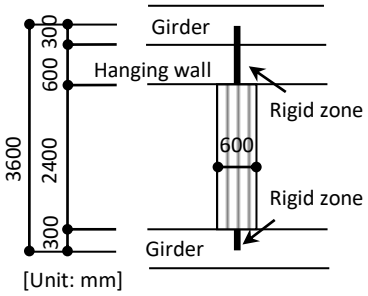

Fig.2 – Idealized column

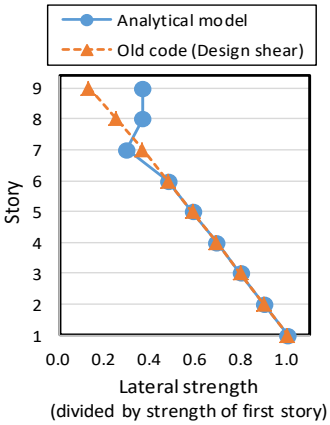

Fig.3 – Story strength distribution (nine-story building)

Table 1 – Structural properties of the analytical models

(a) Three-story building

Story	Weight (kN)	Initial stiffness (kN/cm)	Strength (kN)	*C*	*F*	*1/Ai*	I_S
3	753	3730	1130	1.50	1.0	0.73	1.09
2	753	3730	1130	0.75	1.0	0.87	0.65
1	753	2990	900	0.40	1.0	1.00	0.40

(b) Nine-story building

Story	Weight (kN)	Initial stiffness (kN/cm)	Strength (kN)	*C*	*F*	*1/Ai*	I_S
9	753	1510	1820	2.40	1.0	0.44	1.06
8	753	1510	1820	1.20	1.0	0.55	0.66
7	753	1210	1460	0.65	1.0	0.62	0.40
6	753	1930	2330	0.77	1.0	0.68	0.52
5	753	2300	2780	0.74	1.0	0.74	0.55
4	753	2630	3170	0.70	1.0	0.80	0.56
3	753	3070	3700	0.70	1.0	0.86	0.60
2	753	3510	4230	0.70	1.0	0.93	0.65
1	753	3950	4760	0.70	1.0	1.00	0.70

2.2 Hysteresis model

The relationship between the lateral load and the inter-story drift in the model was represented by a quadrilinear function based on previously conducted collapse tests [4]. The specimens simulating brittle columns were tested under a constant axial load (an axial stress ratio of 0.2). The load was applied until the specimens were unable to sustain it. Three columns, labeled S1, S2, and FS1, were used in the model. The longitudinal bar ratios (p_g), defined as the total main reinforcement areas divided by the column section, were 2.65% for columns S1 and S2 and 1.69% for column FS1. The transverse bar ratios (p_w) were 0.21% for columns S1 and FS1 and 0.14% for column S2. The relationship between the lateral load and inter-story drift obtained using the test results and the analytical models as well as photos taken at collapse are shown in Fig.4. The inter-story drift angle was translated from the drift angle by applying the geometric shape shown in Fig.2. Columns S1 and S2 failed in shear before flexural yielding and lost their axial load-carrying capacity (i.e., collapsed) at an inter-story drift of 8.9% and 3.6%, respectively, whereas column FS1 failed in shear after flexural yielding and collapsed at an inter-story drift of 3.5%.

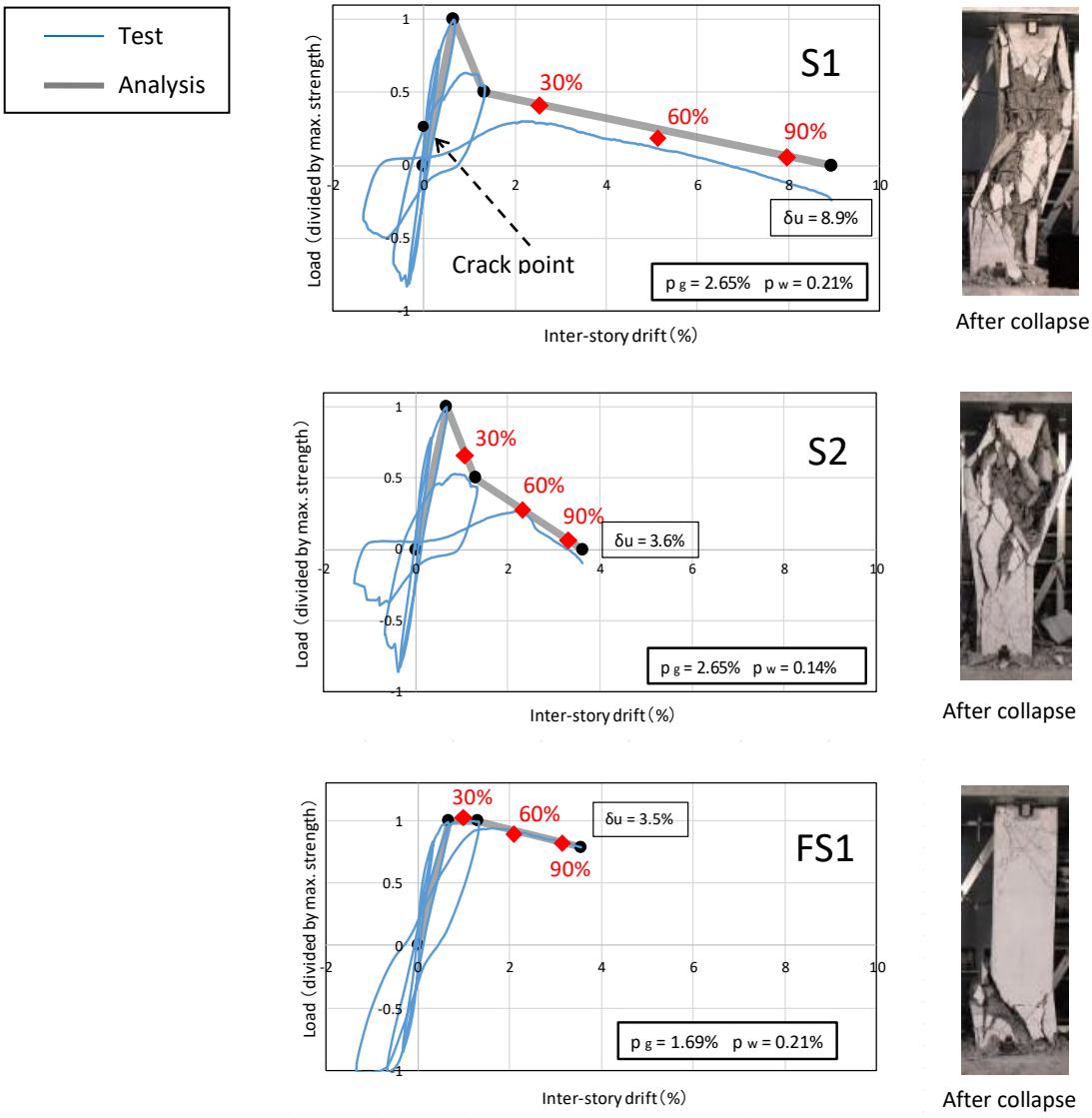

Fig.4 – Load versus drift (collapse story) and damage condition

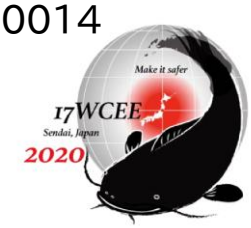

The Takeda-slip model [8] incorporating strength deterioration after maximum load was used in the dynamic analysis (Fig.4). The relationship between lateral load and inter-story drift was represented by a quadrilinear function. The framework prior to maximum loading was the same for the three columns. Loading at the first break point (crack point) was 33% of the maximum load. The inter-story drift at the maximum load was assumed to be uniform for all stories at 0.67%. The inter-story drift at the third break point was assumed to be uniform for all stories at 1.3%. Loading at the third break point for columns S1 and S2 was 50% of the maximum load, while that for column FS1 was 100% of the maximum load. As stated above, the collapse drifts for columns S1, S2, and FS1 were 8.9%, 3.6%, and 3.5%, respectively. Loading at the collapse point was assumed to be zero for columns S1 and S2 and 80% of the maximum load for column FS1. Note that S2 and FS1 had almost the same collapse drift but different types of strength deterioration. The collapse drift was set as uniform for all stories of the three-story building and the top three stories of the nine-story building. However, the drift was reduced proportionally from the third story with decreasing story, taking into consideration the large axial load for these stories. Table 2 shows the collapse drifts of columns S1, S2, and FS1. In Table 2, the highlighted rows indicate the collapse story. Collapse drifts of the collapse stories of the three- and nine-story buildings were the same because their axial loads were the same.

Table 2 – Collapse drift (columns S1, S2, and FS1)

(a) Three-story building

	Story	S1	S2	FS1
	3	8.9%	3.6%	3.5%
	2	8.9%	3.6%	3.5%
Collapse story	1	8.9%	3.6%	3.5%

(b) Nine-story building

Story	S1	S2	FS1
9	8.9%	3.6%	3.5%
8	8.9%	3.6%	3.5%
7	8.9%	3.6%	3.5%
6	8.5%	3.4%	3.4%
5	8.0%	3.2%	3.2%
4	7.6%	3.1%	3.0%
3	7.2%	2.9%	2.8%
2	6.7%	2.7%	2.7%
1	6.3%	2.5%	2.5%

2.3 Dynamic analysis

Viscous damping is proportional to initial stiffness, because if viscous damping proportional to instantaneous stiffness is considered, acceleration (and not damping) results in regions of a negative instantaneous stiffness. The damping ratio was set at 1%. The numerical integration method adopted was Newmark's β method (β = 0.25) [9].

2.4 Ground motions

Eight ground motions recorded during severe past earthquakes were used for the analysis (Table 3; JMA at the 1995 Southern Hyogo Prefecture earthquake, ELC at the 1940 Imperial Valley earthquake, Sendai at the 2011 off the Pacific coast of Tohoku, UTO at the 2016 Kumamoto earthquake, TMK at the 2003 Tokachi-oki earthquake, TKC at the 2003 Tokachi-oki earthquake, KWZ at the 2007 Chuetsu-oki Niigata Prefecture earthquake, and MXC at the 1958 Mexico earthquake). Table 3 shows the maximum ground velocities V_{max} from the original level of ground motions. Note that V_{max} is calculated as the maximum response velocity for an elastic single-degree-of-freedom system with a natural period of 10 s and a damping ratio of 0.707% [10].

Upon conducting the analyses, the level of ground motion was adjusted based on the maximum ground velocity V_{max}. In Japan, such a normalization based on V_{max} is commonly used to evaluate the seismic intensity of earthquake motions in buildings. Fig.5 shows the acceleration spectra for earthquakes with V_{max} of 50 cm/s. In the figure, the damping ratio is 1%. According to Fig.5, the response acceleration spectra of ground motions that rose sharply with a peak less than the natural period of 1.0 s were classified as short-period earthquakes, and those with a peak of more than 1 s were classified as long-period earthquakes (see Table 3).

The levels of the first ground motions were adjusted such that the maximum drift would occur at the maximum strength and 30%, 60%, or 90% of the collapse drift. Each point is shown in Fig.4. The second ground motion (in the same way as the first ground motion) was input successively and the level was adjusted to V_{max} values of 50 cm/s, 75 cm/s, 100 cm/s, 125 cm/s, and 150 cm/s to identify the level necessary to induce collapse. Thus, the relationship between the maximum drift in the first ground motion and the collapse time was discussed.

Table 3 – Ground motions (original level)

Name	Direction	Year, Earthquake, Site	Maximum ground velocity V_{max} (cm/s)	Duration (s)	Short-period or long-period
JMA	NS	1995, Southern Hyogo Prefecture, Japan Meteorological Agency Kobe	82.6	8.3	Short-period
ELC	NS	1940, Imperial Valley, El Centro	33.6	24.4	
Sendai	EW	2011, off the Pacific coast of Tohoku, Japan Meteorological Agency Sendai	31.5	98.0	
UTO	EW	2016, Kumamoto, K-NET Uto	83.2	10.4	
TMK	NS	2003, Tokachi-oki, K-NET Tomakomai	23.4	92.4	Long-period
TKC	NS	2003, Tokachi-oki, Japan Meteorological Agency Tomakomai Sirakaba	16.3	67.0	
KWZ	NS	2007, Chuetsu-oki Niigata Prefecture, K-NET Kashiwazaki	129.1	6.6	
MXC	EW	1985, Mexico, SCT1	60.6	38.9	

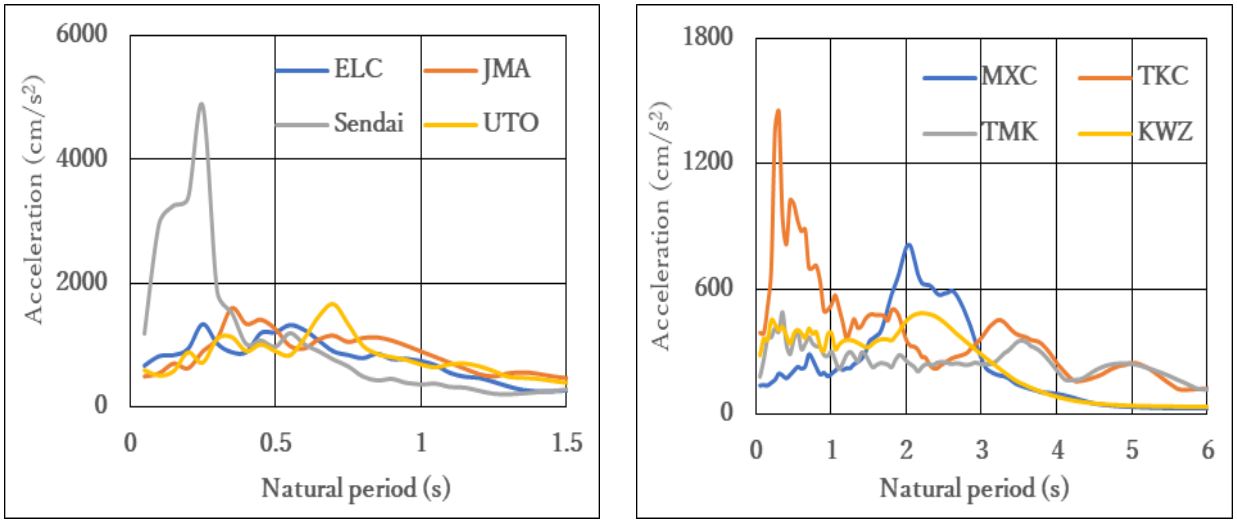

(a)short-period earthquakes (b) long-period earthquakes

Fig.5 – Acceleration spectrum (V_{max} = 50 cm/s)

3. Analytical results

Dynamic analysis was performed for the three columns and various ground motions. The calculations were terminated when the response drift was equal to the collapse drift. The collapse story was computed to suffer the greatest damage in most cases; therefore, the analytical results for the collapse story are as follows.

3.1 Collapse procedure

In this analysis, the ground motion level was adjusted so that the degree of deformation in the first ground motion was the same as it was at maximum strength, and 30%, 60%, 90% of the collapse drift (Fig.4); thus, the collapse time in the second ground motion was obtained. However, in "single (see Fig. 8, 0% of the collapse drift)," only the second ground motion was input for computation, assuming no damage in the first ground motion. Fig.6 shows the time history of the acceleration power (upper), ground acceleration (middle), and inter-story drift (lower). Considering the collapse story for the three-story building with column S2 and the input motion of TMK, in the first ground motion, the maximum inter-story drift was 30% of the collapse drift when the maximum ground velocity V_{max} was 72.5 cm/s. In the second ground motion, the inter-story drift increased, and the building collapsed when V_{max} was 100 cm/s. Here, the duration of seismic motion is the time required for the acceleration power to change from 5% at the end of the earthquake to 95% (Table 3 and Fig.6). The collapse time is defined as the time between the start of the sway at 5% in the second ground motion and collapse. In this case, the collapse time was 20.3 s.

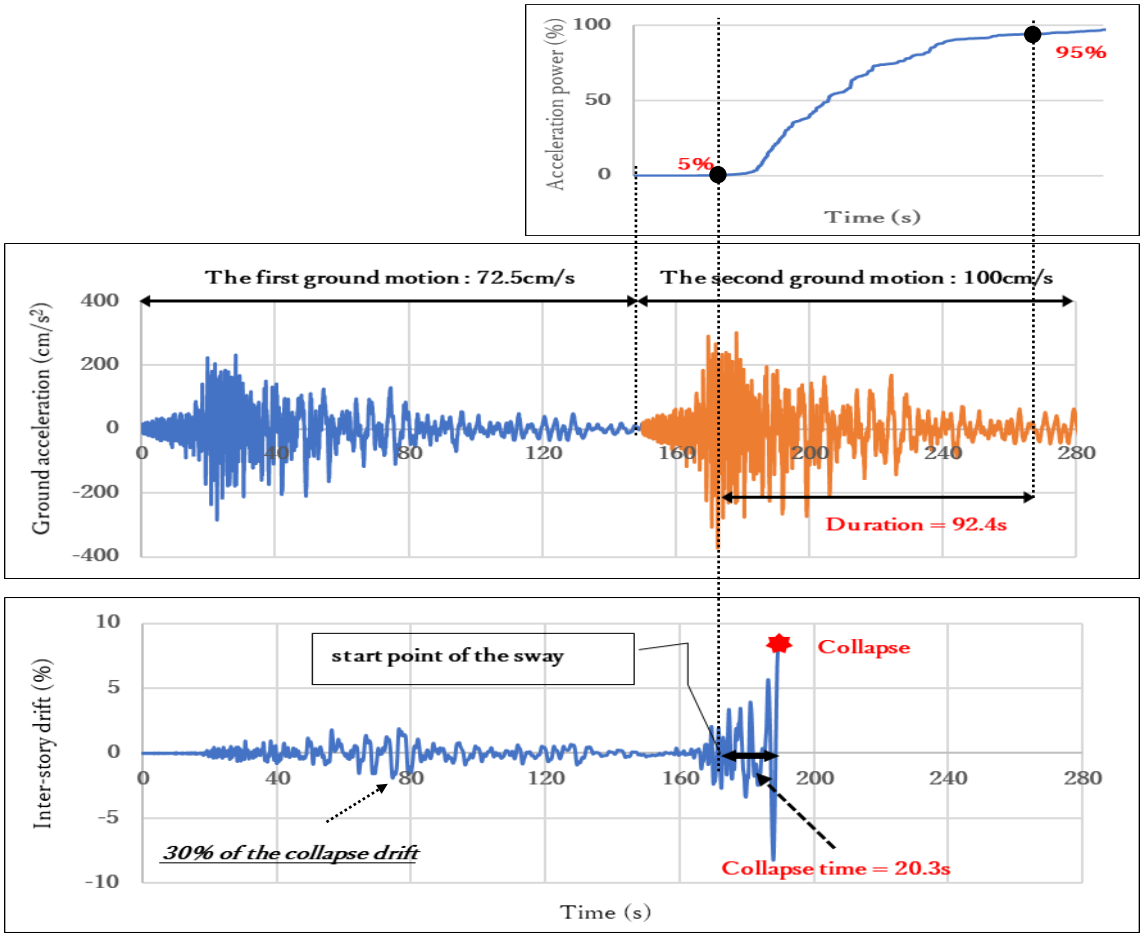

Fig.6 – Time history of acceleration power (upper), ground acceleration (middle), and inter-story drift (lower)

3.2 Relationship between drift level and collapse time

Fig.7 shows the relationship between the maximum drift level of the first ground motion and the collapse time due to the second ground motion (maximum ground velocity = 125 cm/s) for three-story buildings. In addition, the figure shows the results with the short-period earthquakes and long-period earthquakes as input for S1, S2, and FS1 columns. The left-side and the right-side show the results for short- and long-period earthquakes, respectively. If the results cannot be represented as plots, no collapse occurs. The nine-story buildings will be described later.

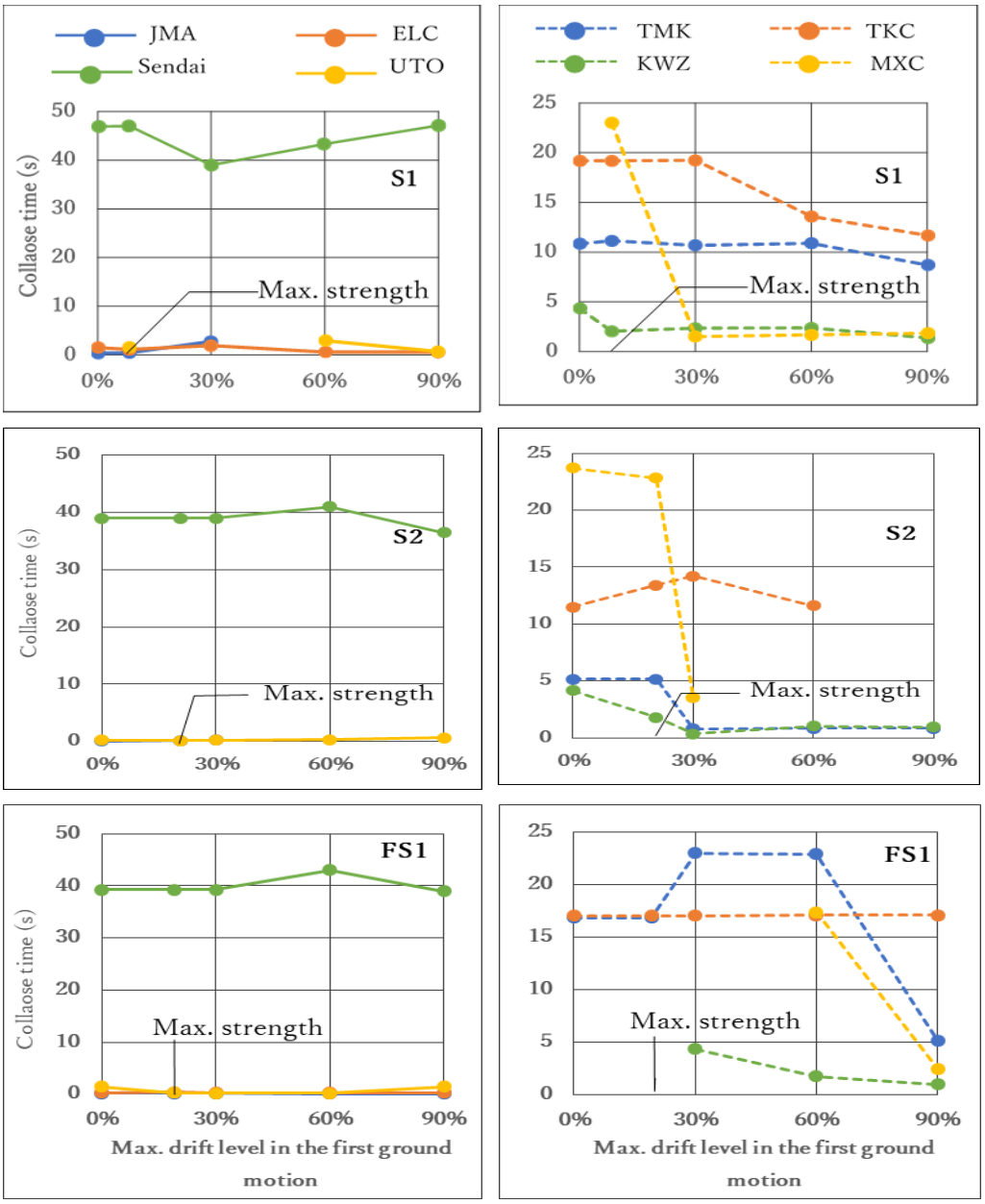

(a) short-period earthquakes (b) long-period earthquakes

Fig. 7 – Maximum drift level in first ground motion and collapse time
(Three-story buildings, V_{max} of the second ground motion= 125 cm/s)

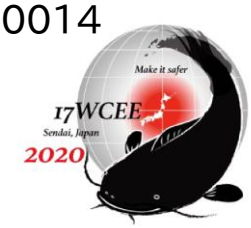

According to Fig. 7, for column S1 and four short-period earthquakes, the collapse times ranged from 0.40 s to 47.1s. Except for ELC, the remaining three ground motions out of the four short-period earthquakes, showed the collapse time increased (harder to collapse) with the increase in maximum drift level in the first ground motion. Conversely, for the four long-period earthquakes, the collapse times ranged from 0.36 s to 23.0 s. When the maximum drift level in the first ground motion increased, the collapse time decreased. This is because a plastic response increases the natural period, and the degree of this increase increases with collapse drift. Thus, column S1 with its large collapse drift has small rigidity and a long natural period after the first ground motion, and it becomes difficult to resonate with the second ground motion of short-period earthquakes and considerably resonates with the long-period ones.

According to column S2, for short-period earthquakes, the collapse times ranged from 0.16 s to 41.0 s. The collapse times were almost same as the maximum drift level in the first ground motion. For long-period earthquakes, the collapse time ranged from 0.36 s to 23.7 s. There was a downward trend toward the right; however, in TMK and KWZ, the collapse time was almost constant for more than 30% of the collapse drift. Because column S2 has the greater strength deterioration and smaller collapse drift than S1, the effect of the collapse drift level in the first ground motion was considered to be small. In addition, regardless of the periodic characteristic, the collapse time of column S2 was considered to be relatively shorter than that of column S1; therefore, it can be said that column S2 collapses more easily than column S1 (this is because the collapse deformation of column S2 was smaller than that of column S1). Moreover, cases without plots where the predetermined deformation were not obtained in the first ground motion.

For column FS1 and short-period earthquakes, the collapse times ranged from 0.15 s to 43.0 s. Sendai tended to rise toward the right; however, in the other three ground motions, collapse drift level that induced the collapse time hardly changed. In contrast, for long-period earthquakes, the collapse times ranged from 0.94 s to 23.0 s. KWZ exhibited a downward trend, but the others exhibited a specific trend. In addition, by comparing the collapse time of columns FS1 and S2, it was found that the collapse time of short-period earthquakes for FS1 were almost the same as that of S2, but that of long-period earthquakes for FS1 were relatively longer than that of S2. This is because columns S2 and FS1 had almost the same collapse drift and different types of strength deterioration.

3.3 Relationship between second ground motion level and collapse time

Fig. 8 shows the relationship between the maximum velocity of the second ground motion and the collapse time when JMA and TMK were input to three-story buildings with columns S1, S2, and FS1. The left-side is JMA, and the right is TMK. The maximum velocity of the second ground motion varied from 50 cm/s to 150 cm/s in intervals of 25 cm/s. Moreover, regardless of the periodic characteristics of the seismic ground motion, the collapse time decreased as the maximum velocity of the second ground motion increased.

According to JMA, column S1 had the shortest collapse time when the collapse drift level in the first ground motion had the maximum strength. Conversely, according to TMK, the collapse time was the shortest when for 90% of the collapse drift. The reason has been discussed above.

For columns S2 and FS1, the collapse time was the shortest for almost all ground motions when the drift level in the first ground motion was 90% of the collapse drift. That is, the collapse drift of S2 and FS1 was small, and it was difficult to affect the drift level in the first ground motion.

3.4 Relationship between the duration and the second ground motion that induced collapse time

Considering column S1 as an example, Fig. 9 shows the relation between the duration of each ground motion and the collapse time in the second ground motion. The maximum velocity of the second ground motion is 100 cm/s in the left part and 125 cm/s in the right, respectively. For almost all ground motions, a longer duration induced a longer collapse time. For the maximum velocity in the second ground motion, which was 125 cm/s, the collapse time for TMK was relatively short. It was different from the result and the reason was difficult to understand. Further, similar results were observed for columns S2 and FS1.

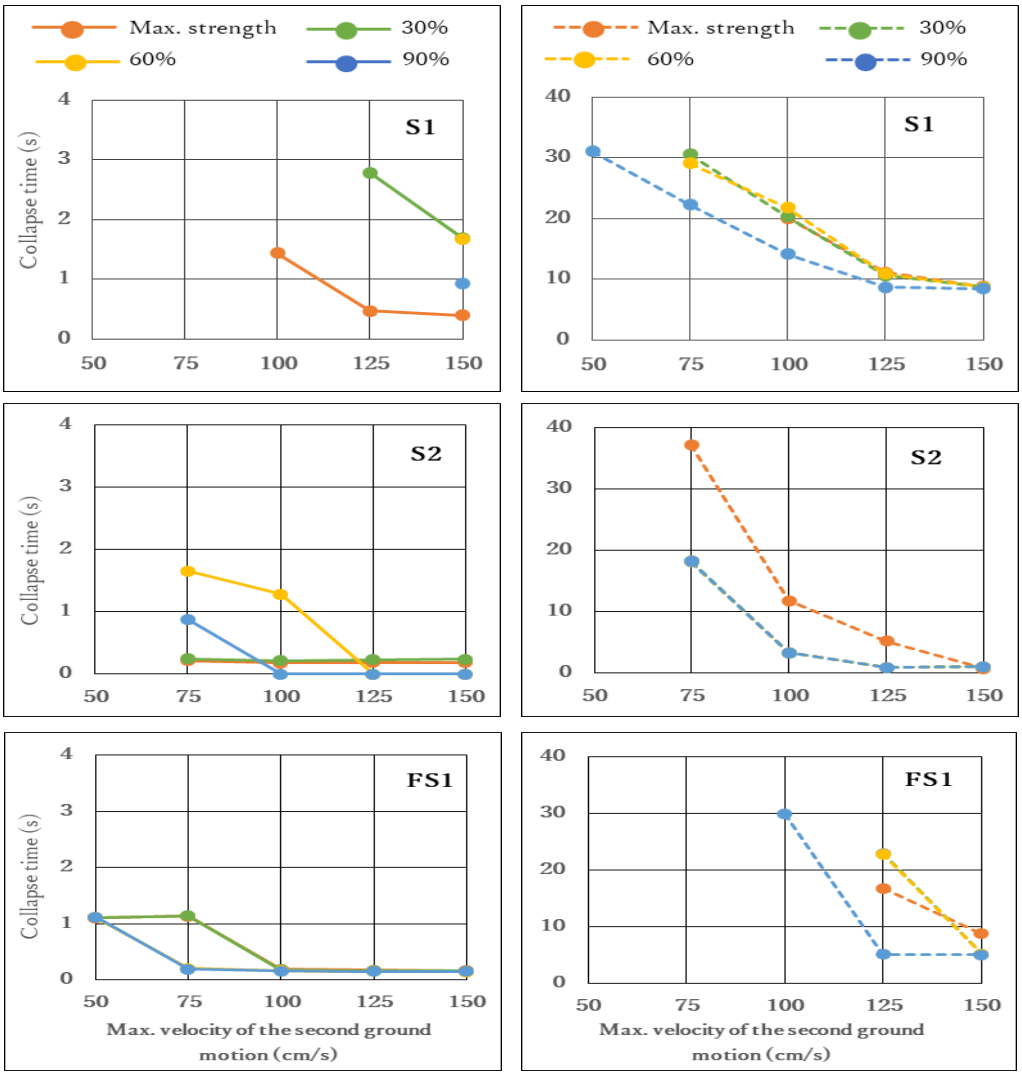

(a) JMA (b) TMK

Fig. 8 – Maximum velocity of second ground motion and collapse time (three-story building)

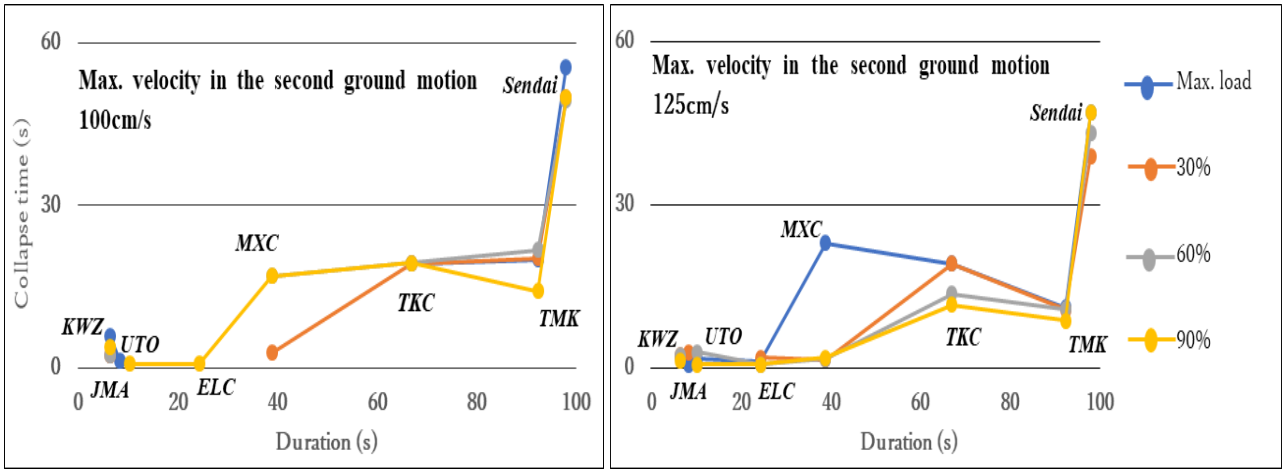

Fig.9 – Duration and collapse time (three-story building, column S1)

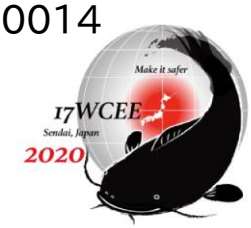

3.5 Effect of number of story on collapse time

Considering JMA and TMK as examples, according to the relationship between the drift level in the first ground motion and V_{max} of the second ground motion (125 cm/s) that induces the collapse time, Fig. 10 shows the comparison of three- and nine-story building. They are indicated by dotted lines and straight lines, respectively. For the nine-story building, the trend of relationship between the drift level in the first ground motion and the collapse time was similar to that of the three-story building. However, the collapse time of the nine-story building was relatively shorter than that of three-story building. This can be because once a collapse story suffers heavy damage, lateral drifts of other stories decrease and concentrate on the collapse story. In other words, the more stories a building has, the larger the maximum drift of the collapse story, and the columns collapse easily [11]. In addition, the nine-story building has a longer natural period than the three-story building; thus, it is easy to resonate with a long-period earthquake such as TMK, and the collapse time is shortened.

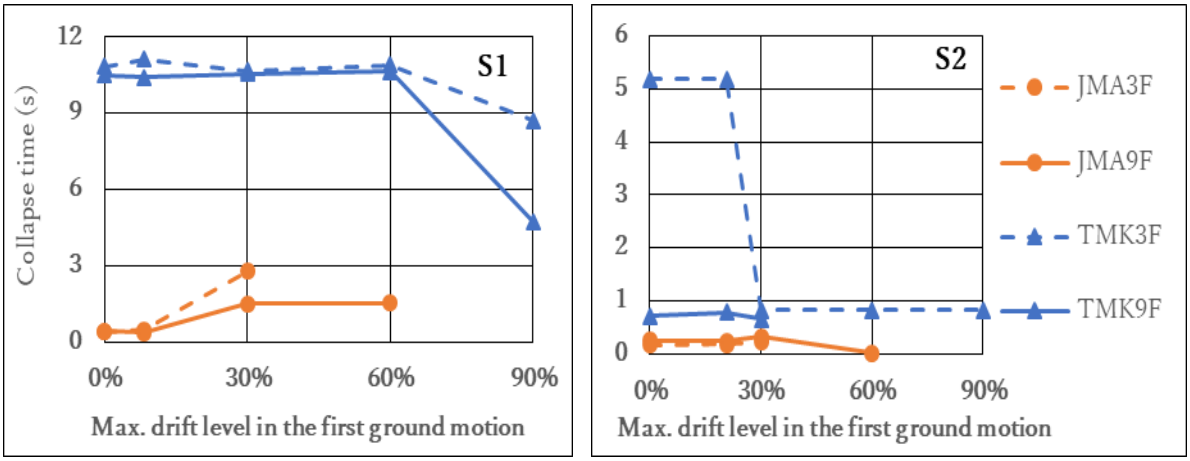

Fig. 10 – Drift level and collapse time (V_{max} of second ground motion = 125 cm/s)

4. Conclusions

(1) According to the maximum drift level of the first ground motion, the longer the deformation, the longer the natural period of the building. In addition, the second ground motion of a long-period earthquake tends to resonate, and the collapse time becomes shorter. However, the opposite results are obtained for a short-period earthquake when the natural period of the building in the first ground motion is longer.

(2) The higher the seismic level of the second ground motion, the shorter the collapse time, regardless of the periodic characteristic.

(3) The longer the duration of the seismic motion, the longer the collapse time.

(4) In a multistory building with a vulnerable story, the deformation of each story concentrates on the collapse stories. Therefore, as the number of stories increases, the concentration of the deformation increases, and the collapse time decreases.

5. Acknowledgments

The ground acceleration records of Uto for the Kumamoto earthquake in 2016, Tomakomai for the off the Pacific coast earthquake of Tohoku in 2011, and Kashiwazaki for the Chuetsu-oki Niigata Prefecture earthquake in 2007 were recorded by K-NET (National Research Institute for Earth Science and Disaster Prevention).

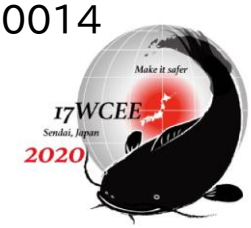

This work was supported by JSPS Grants-in-Aid for Scientific Research Grant: Number 17K06636 and Collaborative Research Projects (CRP)- 2019: Laboratory for Materials and Structures, Institute of Innovative Research, Tokyo Institute of Technology.

6. Appendix

The seismic capacity index *Is* is given as follows [5,6]:

$$Is = E_0 \cdot S_D \cdot T, \quad (1)$$

where S_D is the configuration index (assumed to be 1.0 for this study), T is the time index, (assumed to be 1.0 for this study), and E_0 is determined as follows:

$$E_0 = (1/Ai) \cdot C \cdot F, \quad (2)$$

Where A_i is the vertical distribution factor of story shear coefficients according to Japanese building codes, and i is the story to be studied. The index C is defined as the strength of a column divided by the total weight of the floors above the column, whereas the index F is determined according to the deformability of the column. For the columns in this study, F was calculated to be 1.0.

7. References

[1] Raghunandan M, Liel A B, Ryu H, et al. (2012): Aftershock Fragility Curves and Tagging Assessments for a Mainshock-Damaged Building, Proceedings of the fifteenth World Conference in Earthquake Engineering

[2] Jeon J S, DesRoches R, Brilakis I, and Lowes L N (2012): Aftershock Fragility Curves for Damaged Non-Ductile Reinforced Concrete Buildings, Proceedings of the fifteenth World Conference in Earthquake Engineering

[3] Diaz F M, Kusunoki K, and Tasai A (2013): Analytical Study on the Seismic Performance Estimation using the Equivalent Damping and Response Reduction Ratio for Aftershocks, Journal of Structural Engineering, AIJ and JSCE, Vol. 59B, pp. 399-408

[4] Takaine Y, Nakamura T, and Yoshimura M (2003): *Collapse Drift of Reinforced Concrete Columns*, Journal of Structural and Construction Engineering, Architectural Institute of Japan, No. 573, pp. 153-160 (in Japanese).

[5] Japan Association for Building Disaster Prevention (2001): *Standard for Seismic Evaluation of Existing RC Buildings* (in Japanese)

[6] Otani S (2003): *Seismic Vulnerability Assessment and Retrofit – State of Practice in Japan* -, Proceedings of the fib 2003 Symposium – Concrete Structures in Seismic Regions -, pp. 43-62.

[7] Tamura M and Tanaka A (1999): *Statistical Study on the Evaluation of Seismic Capacity of Existing RC Buildings*, Journal of Structural Engineering, Architectural Institute of Japan, Vol. 45B, pp. 297-304

[8] Eto H and Takeda T (1977): Inelastic Earthquake Response Frame Analysis of Reinforced Concrete Structures, Summaries of Technical Papers of Annual Meeting, Architectural Institute of Japan, pp.1877-1878 (in Japanese)

[9] Newmark N M (1959): *A Method of Computation for Structural Dynamics*, Proc. ASCE, Vol. 85, EM3, pp. 67-94

[10] Evaluation Committee of High-rise Buildings (1986): *Seismic Ground Motion for Dynamic Analysis of High-rise Buildings*, The Building Center of Japan, Building Letter for June, pp. 49-50 (in Japanese)

[11] Nakamura T, Yoshimura M, and Kondo T (2007): Effect of number of stories on the intermediate-story collapse, Proceedings of Japan Concrete Institute, Vol. 29, No. 3, pp. 871-876 (in Japanese)

